Using The Electrical Resistivity Method to Investigate Soil Resistivity at Okokpon, Okada, Edo State, Nigeria

ThankGod Arekumo, Segun Ogunmakinwa & Avery Tonipre Thompson

Department of Physics Federal University Otuoke, Bayelsa State

DOI: https://doi.org/10.51584/IJRIAS.2026.11070072

Received: 17 July 2026; Accepted: 22 July 2026; Published: 03 August 2026

ABSTRACT

Electrical resistivity surveying was used to characterize the shallow subsurface at the ELPS CS2 site in Okokpon, Okada, Edo State, and to assess the implications for buried metallic infrastructure. Measurements were acquired at six vertical electrical sounding (VES) stations with an ABEM SAS 1000 Terrameter, a 12 V battery, four electrodes, connecting cables, a measuring tape, and a GPS receiver. The Schlumberger array was used to inject current and measure the resulting potential difference. Apparent resistivity values were calculated and inverted to obtain layer resistivities to an investigated depth of approximately 10 m. The interpreted resistivity values ranged from 70.1 Ωm to 9708 Ωm. The lower values are consistent with clay-rich or moisture-retaining horizons, whereas the higher values indicate relatively dry lateritic, sandy, or gravelly materials. Surface and 5 m contour maps also reveal marked lateral variation, including comparatively conductive zones around ERT1, ERT3, and ERT6 and highly resistive zones around ERT4 and ERT5. Overall, the site is not dominated by highly conductive soil; therefore, the resistivity data alone do not indicate a general requirement for cathodic protection. This conclusion should, however, be verified with seasonal measurements and complementary soil-corrosivity parameters before final pipeline design.

Keywords: electrical resistivity, soil corrosivity, vertical electrical sounding, lithology, pipeline corrosion, cathodic protection

INTRODUCTION

Electrical resistivity surveying characterizes soils and rocks by measuring their opposition to electrical current. It is widely applied in geotechnical engineering, environmental assessment, and hydrogeology [1]. Soil resistivity responds to mineral composition, pore-water content, salinity, porosity, and degree of saturation [2]. During a direct-current survey, current is introduced through two electrodes and the resulting potential difference is measured across two additional electrodes. Ohm's law and the electrode geometry are then used to calculate apparent resistivity [3]. Because changes in lithology and saturation can produce strong resistivity contrasts, the method is particularly useful for mapping shallow subsurface heterogeneity [4].

Okokpon in the Okada area of Edo State presents a site-specific interpretation challenge because the shallow geology includes lateritic clay, clayey sand, sand, gravelly or pebbly sand, and discontinuous clay horizons associated with the Benin and Ogwashi-Asaba formations [5]-[7]. These materials can have overlapping electrical responses when their moisture conditions differ. The seasonally wet environment and local groundwater movement may further reduce soil resistivity during periods of high saturation, potentially increasing the apparent corrosion susceptibility of buried metallic facilities. A single regional description is therefore insufficient for engineering decisions at the ELPS CS2 site.

The novelty of this study lies in combining six Schlumberger VES soundings, one-dimensional layer inversion, and spatial contouring at the surface and at 5 m depth to evaluate lithological variability and its implications for pipeline corrosion at a specific infrastructure location in Edo State. Unlike a general geological appraisal, the survey identifies local conductive and resistive pockets that could influence the placement and protection of buried oil and gas pipelines, water pipes, cables, and other conductive facilities. The study therefore aims to determine the vertical and lateral distribution of soil resistivity to approximately 10 m depth and to provide a more defensible site-specific basis for corrosion-risk assessment.

Description of the Work

Electrical resistivity measurements were acquired at six stations across the ELPS CS2 site in Okokpon, Okada, Edo State. Figure 1 shows the survey layout, while Table 1A presents the station coordinates. The survey was designed to determine the lateral and vertical distribution of soil resistivity from the ground surface to the investigated depth. At each station, current was introduced through the outer electrodes, and the resulting potential difference was measured across the inner electrodes. The resulting resistance data were used to calculate apparent resistivity and characterize the electrical properties of the subsurface.

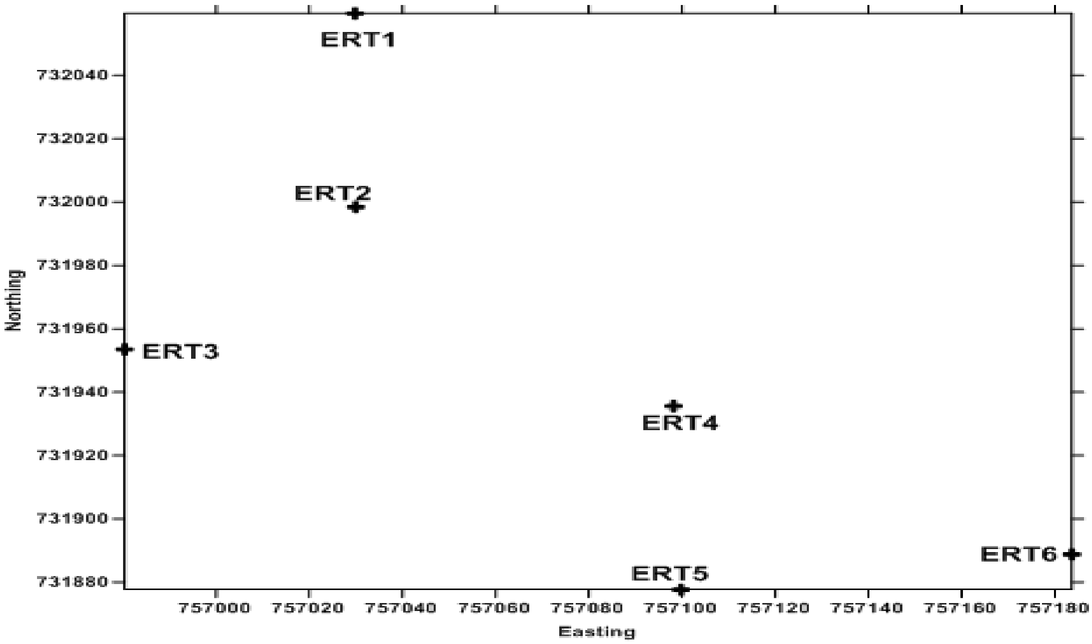

Figure 1: Work layout showing the electrical resistivity test locations.

Table 1A**:** Electrical resistivity test locations and coordinates

Electrical Points	Coordinates	
	Easting	Northing
ERT1 (RT1)	757029.83	732059.59
ERT2 (RT2)	757030.01	731998.52
ERT3 (RT3)	756980.40	731953.56
ERT4 (RT4)	757098.20	731935.64
ERT5 (RT5)	757099.78	731877.69
ERT6 (RT6)	757183.66	731888.87

General Geology and Hydrology of the Work Area

More than 80% of Edo State is underlain by Cretaceous to Tertiary sedimentary formations. The study area contains sediments associated with the Anambra Basin and the Niger Delta sequence, including clay-bearing units. The Ogwashi-Asaba Formation, also referred to as the Azagba-Ogwashi Formation, comprises alternating clay, sand, grit, lignite seams, and gritty clay and grades upward into the Benin Formation. It is exposed in stream channels in the northern Benin region, west of Ekiadolor-Iwu, east of Utekon, and north of Azalla [5].

The Benin Formation is generally assigned an Oligocene to Pleistocene, and locally Recent, age [6]. Its upper section commonly consists of reddish to reddish-brown lateritic, indurated clay and sand, underlain by more friable pinkish, yellowish, or whitish gravelly and pebbly sands, clayey soils, sands, and clay [7]. The sequence is poorly bedded and contains discontinuous clay horizons at different depths. The formation is estimated to be about 800 m thick beneath Benin City and approximately 1,830 m thick near the coast, with exposures in erosion sites, sand quarries, and road cuttings.

Regionally, the Imo Shale overlies the Nsukka Formation and represents a shallow-marine shelf setting with preserved foreshore and shoreface sands [8]. It contains black shale, blue-grey clay, marl, calcareous sandstone, and limestone [9]. Eocene regression produced the Ameki and Nanka formations [10], [11], while the Agbada and Akata formations represent prograding shoreface or river-plain deposits and their marine equivalents in the northern Niger Delta. The Oligocene to Recent Ogwashi-Asaba and Benin formations dominate the upper part of the local stratigraphic succession [12]. The alternating permeable sands and less permeable clay horizons can create localized infiltration, perched saturation, and groundwater contrasts. These hydrological variations are relevant because they can temporarily lower soil resistivity, particularly during wet periods [2], [7].

Materials and Methods

Electrical resistivity data were acquired with the Schlumberger configuration at the six predetermined stations. Four electrodes were inserted into the ground according to the selected AB/2 and MN/2 spacings. The two outer electrodes served as current electrodes, while the two inner electrodes measured the potential difference. Connecting cables linked the electrodes to the ABEM SAS 1000 Terrameter, which was powered by a 12 V battery. After the instrument had completed its start-up and configuration procedures, the subsurface resistance (Ω) was measured and recorded. The spacing between the current electrodes was progressively increased while the potential-electrode spacing was kept constant until the required spread length and investigation depth were achieved.

Data Processing

Field resistance values, measured in ohms (Ω), were entered into a spreadsheet. The appropriate Schlumberger geometric factor, K, was applied to convert each resistance measurement to apparent resistivity in ohm-metres (Ωm), as reported in Tables 1 to 6. The apparent resistivity data were then inverted to estimate the resistivity, thickness, and depth of the subsurface layers. The resulting one-dimensional models were plotted on logarithmic axes (Figures 1 to 6). The interpreted resistivity values at the surface and at 5 m depth were subsequently interpolated to produce the contour maps in Figures 7 and 8 and the corresponding values in Tables 7 and 8.

Results

The one-dimensional models in Figures 1 to 6 indicate interpreted resistivity values ranging from 70.1 Ωm to 9708 Ωm within the upper 10 m. ERT1 and ERT2 generally begin with high near-surface resistivity and show an overall decrease with depth. ERT3 to ERT6 display more variable profiles, with alternating low- and high-resistivity layers. This vertical fluctuation indicates a heterogeneous sequence rather than a uniform soil column.

The surface values used for the contour map range from 635 Ωm at ERT6 to 9306 Ωm at ERT5. At 5 m depth, the values range from 121 Ωm at ERT3 to 9613 Ωm at ERT5. ERT1 decreases from 1253 Ωm at the surface to 234 Ωm at 5 m, ERT2 decreases from 7977 Ωm to 4230 Ωm, and ERT3 decreases from 2489 Ωm to 121 Ωm. In contrast, ERT4 increases from 3328 Ωm to 9240 Ωm and ERT5 increases from 9306 Ωm to 9613 Ωm, while ERT6 decreases from 635 Ωm to 373 Ωm. The contour maps therefore delineate relatively conductive zones in the northern, western, and eastern parts of the site and highly resistive zones in the south-central sector.

ISSN No. 2454-6194 | DOI: 10.51584/IJRIAS |Volume XI Issue VII July 2026

Table 1: ELPS CS2 ERT1 (RT1), VES, Current Electrode spacing, Potential Electrode Spacing, Measured Resistance, and calculated Apparent Resistivity (Ωm) for Schlumberger Electrical Resistivity Method.

Depth (m)	AB/2 (m)	Mn/2 (m)	Resistance (Ω)	Apparent Resistivity (Ωm)
0.3	1	0.5	151.91	477.4314286
0.4	1.5	0.5	52.824	373.5411429
0.6	2	0.5	32.739	411.5760000
1.0	3	0.5	18.35	519.0428571
1.5	5	0.5	8.3442	655.6157143
2.0	7	1.5	14.287	733.3993333
3.0	10	1.5	5.7855	606.1000000
5.0	15	3	4.0862	481.5878571
6.0	20	3	1.279	267.9809524
8.0	25	3	0.42457	138.9961310
9.0	30	3	0.31673	149.3155714
10	35	3	0.10413	66.81675000

Figure 1: ELPS CS2 ERT1 VES, Schlumberger 1D electrical resistivity model showing resistivity (ρ), layer thickness (h), and depth (d).

ISSN No. 2454-6194 | DOI: 10.51584/IJRIAS |Volume XI Issue VII July 2026

Table 2: ELPS CS2 ERT2 (RT2), VES, Current Electrode spacing, Potential Electrode Spacing, Measured Resistance, and calculated Apparent Resistivity (Ωm) for Schlumberger Electrical Resistivity Method.

Depth (m)	**AB/2 (m)**	**Mn/2 (m)**	**Resistance (Ω)**	**Apparent Resistivity** (Ωm)
0.3	1	0.5	433.61	1362.774286
0.4	1.5	0.5	152.92	1081.362857
0.6	2	0.5	85.688	1077.220571
1.0	3	0.5	39.008	1103.369143
1.5	5	0.5	15.604	1226.028571
2.0	7	1.5	28.094	1442.158667
3.0	10	1.5	13.985	1465.095238
5.0	15	3	10.913	1286.175000
6.0	20	3	4.7174	988.4076190
8.0	25	3	2.1225	694.8660714
9.0	30	3	1.0036	473.1257143
10	35	3	0.47343	303.7842500

Figure 2: ELPS CS2 ERT2 VES, Schlumberger 1D electrical resistivity model showing resistivity (ρ), layer thickness (h), and depth (d).

ISSN No. 2454-6194 | DOI: 10.51584/IJRIAS |Volume XI Issue VII July 2026

Table 3: ELPS CS2 ERT3 (RT3), VES, Current Electrode spacing, Potential Electrode Spacing, Measured Resistance, and calculated Apparent Resistivity (Ωm) for Schlumberger Electrical Resistivity Method.

Depth (m)	AB/2 (m)	Mn/2 (m)	Resistance (Ω)	Apparent Resistivity (Ωm)
0.3	1	0.5	359.79	1130.768571
0.4	1.5	0.5	100.33	709.4764286
0.6	2	0.5	42.856	538.7611429
1.0	3	0.5	19.865	561.8957143
1.5	5	0.5	12.229	960.8500000
2.0	7	1.5	19.185	984.8300000
3.0	10	1.5	9.0224	945.2038095
5.0	15	3	10.585	1247.517857
6.0	20	3	2.2878	479.3485714
8.0	25	3	5.4328	1778.595238
9.0	30	3	0.59965	282.6921429
10	35	3	1.3071	838.7225000

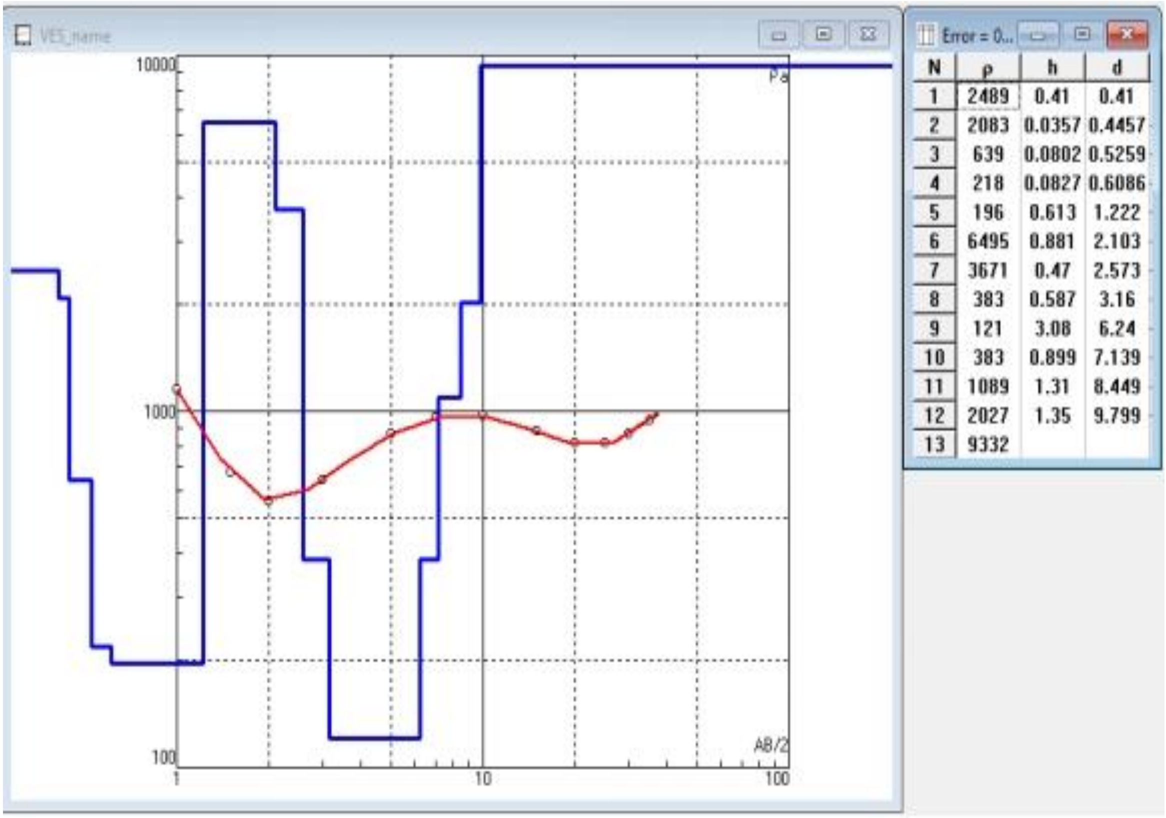

Figure 3: ELPS CS2 ERT3 VES, Schlumberger 1D electrical resistivity model showing resistivity (ρ), layer thickness (h), and depth (d).

ISSN No. 2454-6194 | DOI: 10.51584/IJRIAS |Volume XI Issue VII July 2026

Table 4: ELPS CS2 ERT4 (RT4), VES, Current Electrode spacing, Potential Electrode Spacing, Measured Resistance, and calculated Apparent Resistivity (Ωm) for Schlumberger Electrical Resistivity Method.

Depth (m)	AB/2 (m)	Mn/2 (m)	Resistance (Ω)	Apparent Resistivity (Ωm)
0.3	1	0.5	710.84	2234.068571
0.4	1.5	0.5	280.19	1981.343571
0.6	2	0.5	133.3	1675.771429
1.0	3	0.5	55.192	1561.145143
1.5	5	0.5	16.908	1328.485714
2.0	7	1.5	14.981	769.0246667
3.0	10	1.5	15.189	1591.228571
5.0	15	3	9.8772	1164.098571
6.0	20	3	9.4259	1974.950476
8.0	25	3	3.5358	1157.553571
9.0	30	3	11.592	5464.800000
10	35	3	3.9564	2538.690000

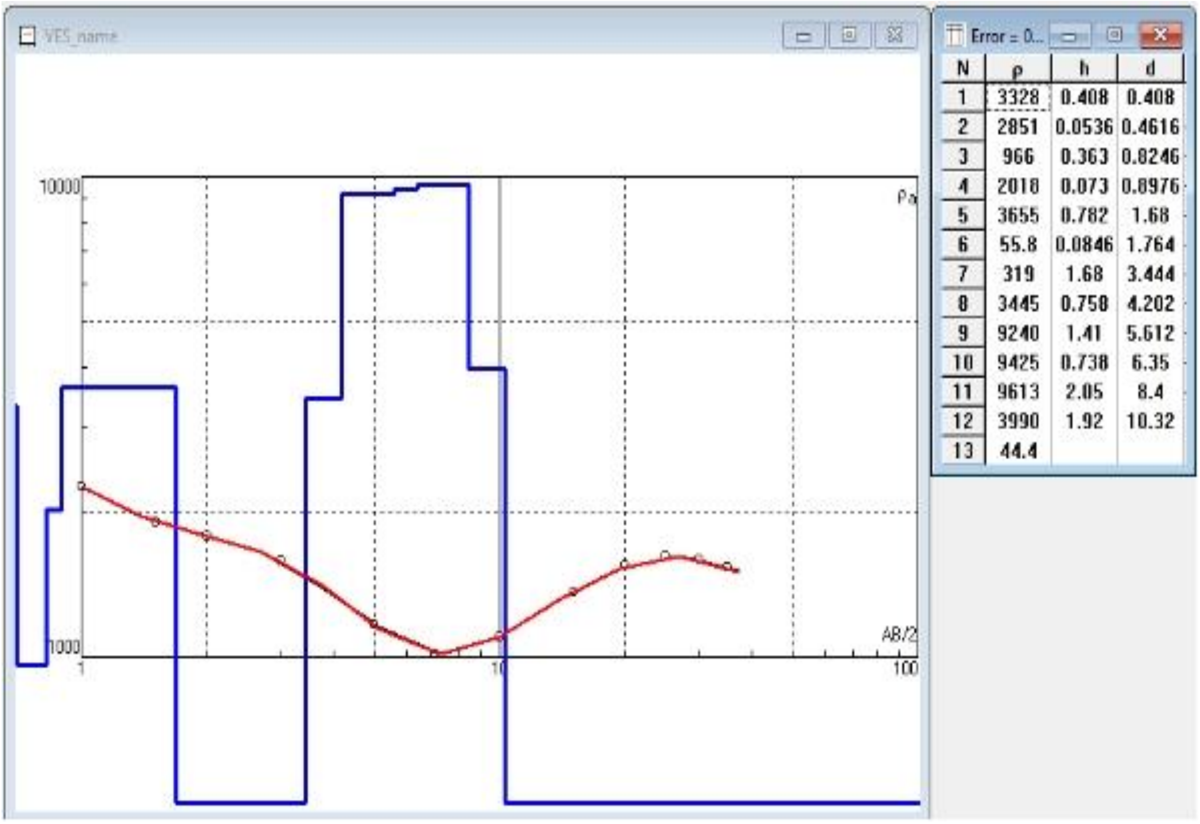

Figure 4: ELPS CS2 ERT4 VES, Schlumberger 1D electrical resistivity model showing resistivity (ρ), layer thickness (h), and depth (d).

ISSN No. 2454-6194 | DOI: 10.51584/IJRIAS |Volume XI Issue VII July 2026

Table 5: ELPS CS2 ERT5 (RT5), VES, Current Electrode spacing, Potential Electrode Spacing, Measured Resistance, and calculated Apparent Resistivity (Ωm) for Schlumberger Electrical Resistivity Method.

Depth (m)	AB/2 (m)	Mn/2 (m)	Resistance (Ω)	Apparent Resistivity (Ωm)
0.3	1	0.5	480.02	1508.634286
0.4	1.5	0.5	155.32	1098.334286
0.6	2	0.5	83.415	1048.645714
1.0	3	0.5	36.789	1040.603143
1.5	5	0.5	15.405	1210.392857
2.0	7	1.5	9.2327	473.9452667
3.0	10	1.5	16.423	1720.504762
5.0	15	3	17.981	2119.189286
6.0	20	3	10.063	2108.438095
8.0	25	3	6.1965	2028.616071
9.0	30	3	3.8069	1794.681429
10	35	3	3.129	2007.775000

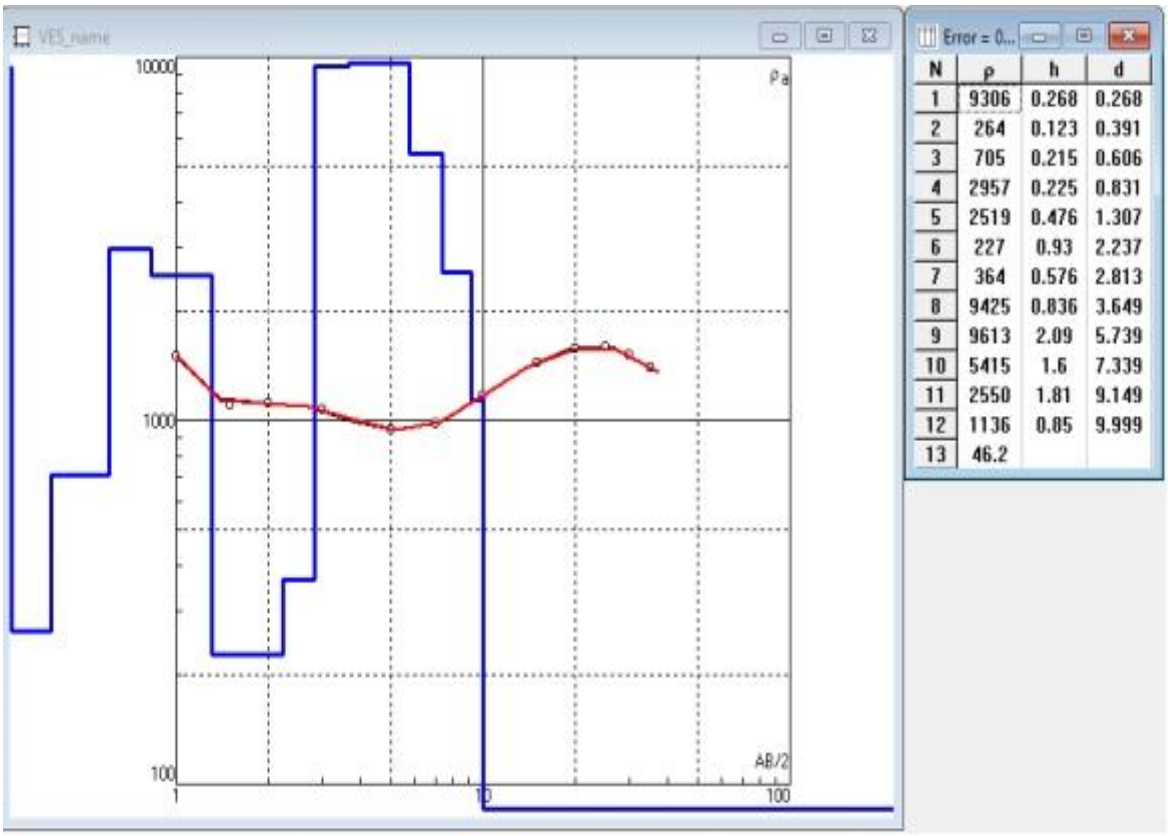

Figure 5: ELPS CS2 ERT5 VES, Schlumberger 1D electrical resistivity model showing resistivity (ρ), layer thickness (h), and depth (d).

ISSN No. 2454-6194 | DOI: 10.51584/IJRIAS |Volume XI Issue VII July 2026

Table 6: ELPS CS2 ERT6 (RT6), VES, Current Electrode spacing, Potential Electrode Spacing, Measured Resistance, and calculated Apparent Resistivity (Ωm) for Schlumberger Electrical Resistivity Method.

Depth (m)	**AB/2 (m)**	**Mn/2 (m)**	**Resistance (Ω)**	**Apparent Resistivity** (Ωm)
0.3	1	0.5	360.71	1133.660000
0.4	1.5	0.5	151.29	1069.836429
0.6	2	0.5	61.769	776.5245714
1.0	3	0.5	26.327	744.6780000
1.5	5	0.5	11.959	939.6357143
2.0	7	1.5	24.229	1243.755333
3.0	10	1.5	12.252	1283.542857
5.0	15	3	11.99	1413.107143
6.0	20	3	6.613	1385.580952
8.0	25	3	4.1885	1371.235119
9.0	30	3	2.8737	1354.744286
10	35	3	2.0582	1320.678333

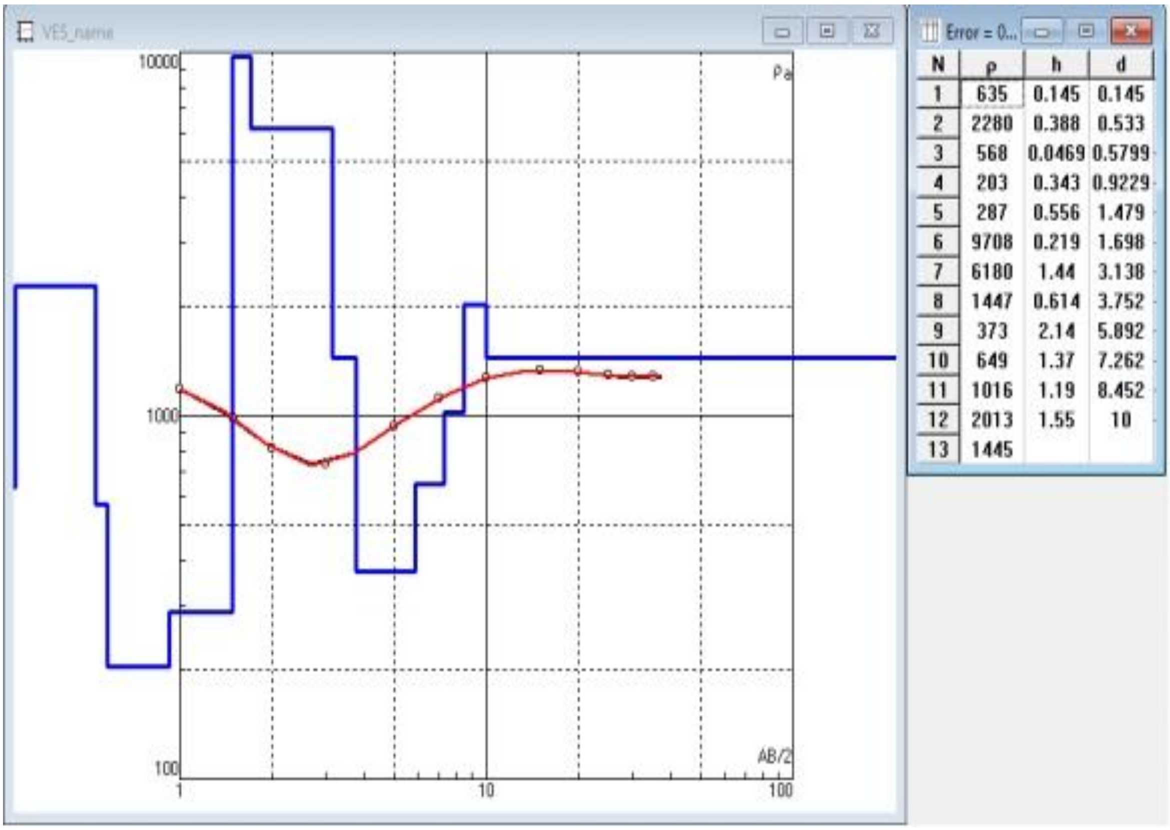

Figure 6: ELPS CS2 ERT6 VES, Schlumberger 1D electrical resistivity model showing resistivity (ρ), layer thickness (h), and depth (d).

ISSN No. 2454-6194 | DOI: 10.51584/IJRIAS |Volume XI Issue VII July 2026

Table 7: Coordinates and electrical resistivity values used for the surface contour map.

Electrical Points	Coordinates		Electrical Resistivity Values in (Ωm)
	Easting	Northing	
ERT1 (RT1)	757029.83	732059.59	1253
ERT2 (RT2)	757030.01	731998.52	7977
ERT3 (RT3)	756980.40	731953.56	2489
ERT4 (RT4)	757098.20	731935.64	3328
ERT5 (RT5)	757099.78	731877.69	9306
ERT6 (RT6)	757183.66	731888.87	635

Electrical resistivity at surface

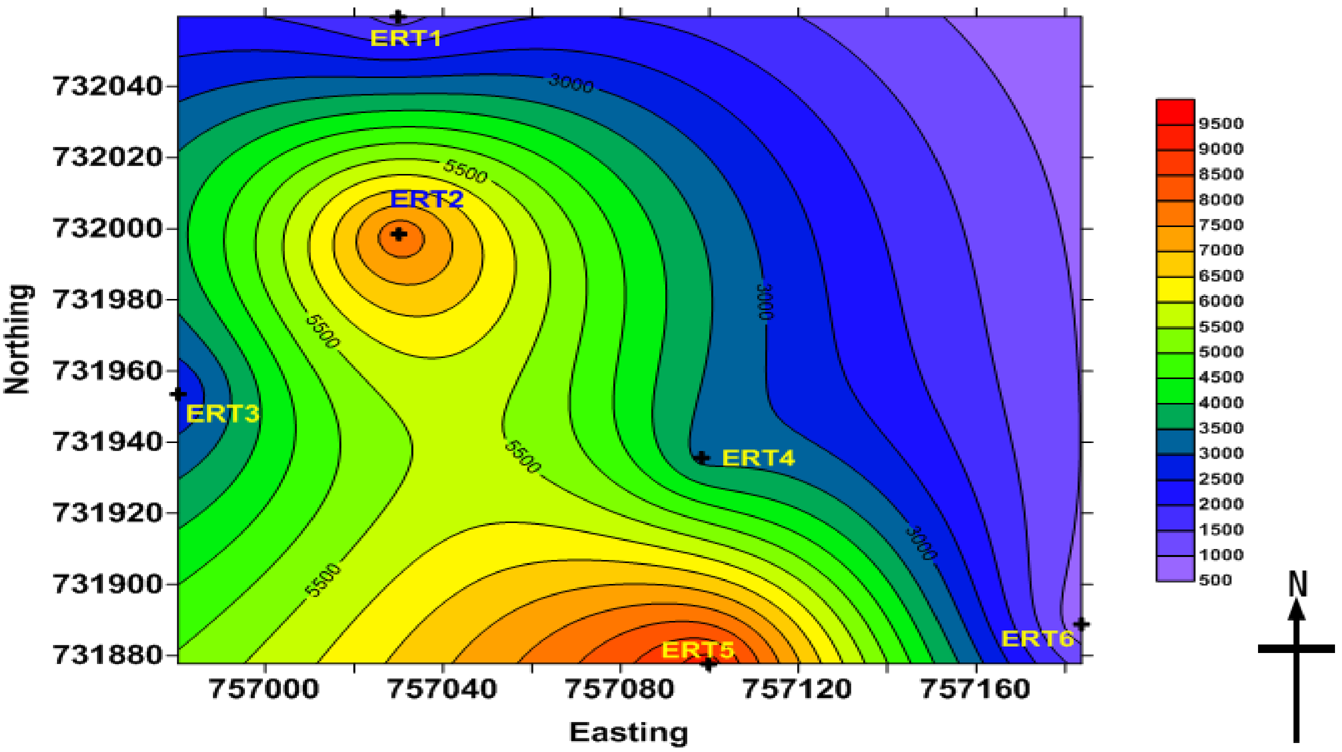

Figure 7: 3D contour of electrical resistivity distribution at the ground surface.

Table 8: Coordinates and electrical resistivity values used for the contour map at 5 m depth.

Electrical Points	Coordinates		Electrical Resistivity Values in (Ωm)
	Easting	Northing	
ERT1 (RT1)	757029.83	732059.59	234
ERT2 (RT2)	757030.01	731998.52	4230
ERT3 (RT3)	756980.40	731953.56	121

ERT4 (RT4)	757098.20	731935.64	9240
ERT5 (RT5)	757099.78	731877.69	9613
ERT6 (RT6)	757183.66	731888.87	373

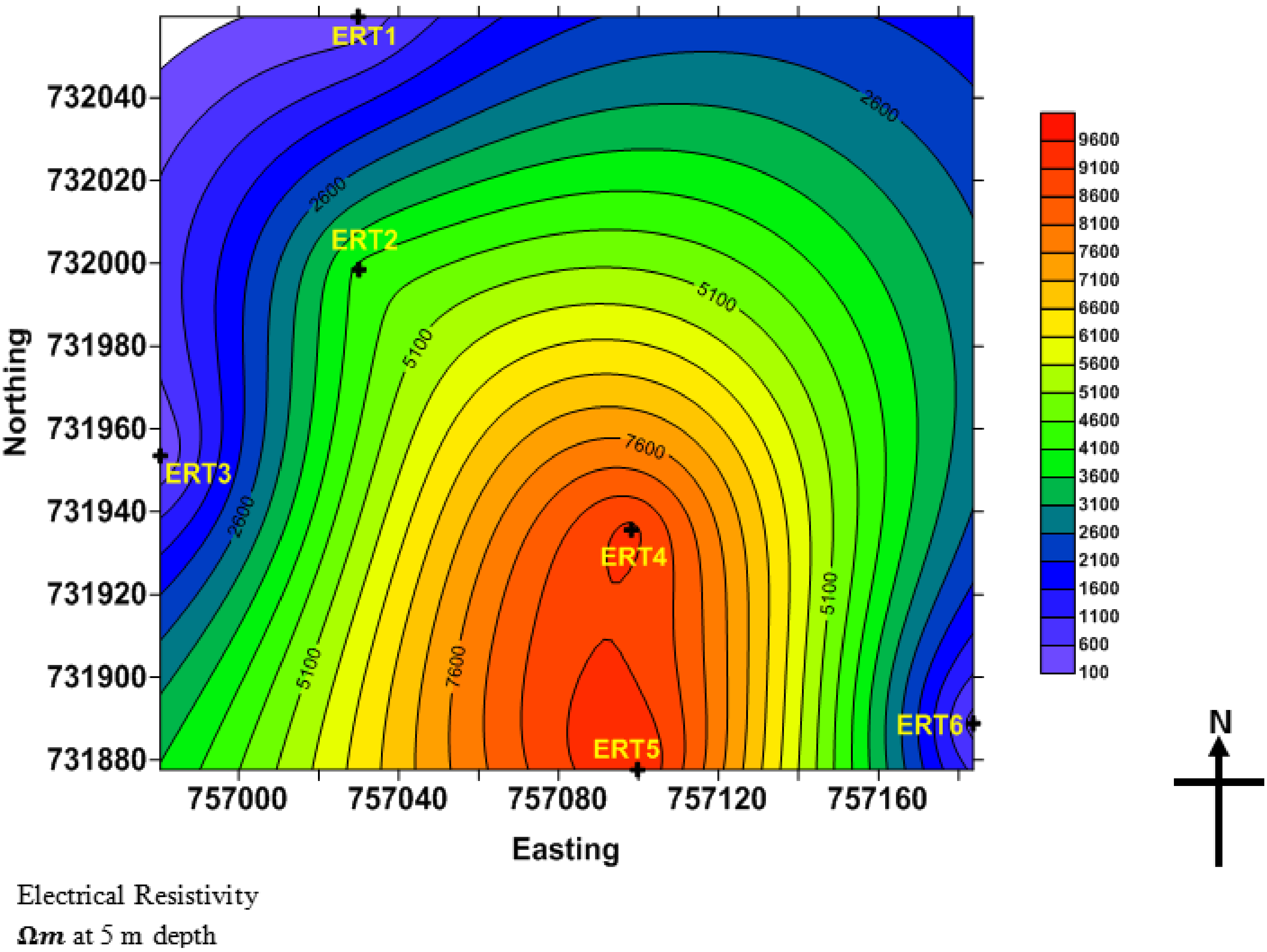

Figure 8: 3D contour of electrical resistivity distribution at 5 m depth.

DISCUSSION AND INTERPRETATION OF THE RESULTS

The resistivity patterns are consistent with the heterogeneous lithology described for the Benin and Ogwashi-Asaba formations. Within this site, values near the lower end of the interpreted range, approximately 70.1 to 400 Ωm, are most plausibly associated with clay-rich, clayey, or strongly moisture-retaining horizons. Clay minerals provide large surface areas for ionic conduction, and fine-grained layers commonly retain more pore water than clean sand. This interpretation is supported by the marked reductions at ERT1, ERT3, and ERT6 at 5 m depth, where values of 234 Ωm, 121 Ωm, and 373 Ωm, respectively, may indicate clayey sand, sandy clay, or locally saturated material. These correlations are interpretive rather than unique because moisture content and pore-water chemistry can cause different lithologies to produce similar resistivity values [2], [4].

Intermediate values, broadly between 400 Ωm and 2000 Ωm, are compatible with mixed lateritic soil, clayey sand, partially saturated sand, or weathered sandy material. Many layers at the six stations fall within this interval, which agrees with the reported alternation of clay, sand, and lateritic horizons. The decreasing trends at ERT1 and ERT2 suggest that relatively dry or compact near-surface materials overlie progressively wetter or more clay-rich units. The alternating profiles at ERT3 to ERT6 are also consistent with discontinuous clay lenses within sandy or gravelly deposits.

Values greater than about 2000 Ωm, including the upper range of 9708 Ωm, are consistent with comparatively dry, coarse-grained sand, gravelly or pebbly sand, and strongly indurated lateritic material. The high resistivity at ERT4 and ERT5 at 5 m depth, 9240 Ωm and 9613 Ωm, respectively, suggests a south-central zone dominated by drier and more permeable sandy or lateritic materials rather than continuous saturated clay. ERT2 also remains relatively resistive at 5 m, although its decline from the surface indicates increasing moisture, finer material, or both with depth. These site-specific interpretive bands should not be treated as universal lithological thresholds; they are most useful when evaluated alongside the local geological description and the relative contrasts among stations.

From a corrosion perspective, the predominance of moderate to high resistivity indicates that most of the surveyed soil is not highly conductive and would generally provide a less favourable electrolyte for galvanic corrosion than very low-resistivity soil. The result therefore does not indicate a site-wide need for cathodic protection based on resistivity alone. However, the lowest-resistivity pockets, particularly around ERT1, ERT3, and ERT6 at depth, deserve closer assessment because buried pipelines may cross localized clay-rich or seasonally saturated zones. A final corrosion-control decision should combine resistivity with pipeline material, coating condition, design life, stray-current exposure, and soil measurements such as pH, chloride, sulphate, redox potential, and microbial activity.

CONCLUSION

The survey identified a heterogeneous shallow subsurface at the ELPS CS2 site, with interpreted resistivity values ranging from 70.1 Ωm to 9708 Ωm in the upper 10 m. Lower values are consistent with clay-rich, clayey-sand, or moisture-retaining horizons, while the highest values are compatible with relatively dry sand, gravelly sand, and indurated lateritic material. The 5 m map distinguishes conductive zones near ERT1, ERT3, and ERT6 from highly resistive zones near ERT4 and ERT5. Because most measured values indicate moderate to high resistivity, the site is not characterized by widespread highly conductive soil. Accordingly, the resistivity results alone do not show a general requirement for cathodic protection; nevertheless, localized low-resistivity zones should be investigated before pipeline installation. Seasonal repeat measurements and complementary soil-corrosivity tests are recommended before the final corrosion-control strategy is selected.

REFERENCES

1. Dahlin, T. (2001). The development of DC resistivity imaging techniques. Computers & Geosciences, 27(9), 1019-1029.
2. Samouëlian, A., Cousin, I., Tabbagh, A., Bruand, A., & Richard, G. (2005). Electrical resistivity survey in soil science: A review. Soil and Tillage Research, 83(2), 173-193.
3. Griffiths, D. H., & Barker, R. D. (1993). Two-dimensional resistivity imaging and modeling in areas of complex geology. Journal of Applied Geophysics, 29(3-4), 211-226.
4. Loke, M. H. (2004). Tutorial: 2-D and 3-D electrical imaging surveys. Geotomo Software.
5. Reyment, R. A. (1965). Aspects of the geology of Nigeria. Ibadan University Press.
6. Short, K. C., & Stauble, A. J. (1967). Outline of the geology of Onitsha, Owerri and Benue provinces. Geological Survey of Nigeria, Bulletin No. 21.
7. Akujieze, C. N. (2004). Effects of anthropogenic activities (sand quarrying and waste disposal) on urban groundwater system and aquifer vulnerability assessment in Benin City, Edo State, Nigeria. PhD Thesis, University of Benin, Benin City, Nigeria.
8. Petters, S. W., & Ekweozor, C. M. (1981). Origin of Cretaceous black shales in the Benue Trough, Nigeria. Journal of Palaeogeography, Palaeoclimatology, Palaeoecology, 40, 311-319.
9. Onyekuru, S. O., Iwuoha, P. O., Iwuagwu, C. J., Nwozor, K. K., & Opara, K. D. (2018). Mineralogical and geochemical properties of clay deposits in parts of Southeastern Nigeria. International Journal of Physical Sciences, 13(14), 217-229.

ISSN No. 2454-6194 | DOI: 10.51584/IJRIAS |Volume XI Issue VII July 2026

10. Obrike, S. E., Osadebe, C. C., & Onyeobi, T. U. S. (2007). Mineralogical, geochemical, physical and industrial characteristics of shale from Okada area, southwestern Nigeria. Journal of Mining and Geology, 43(2), 109-116.
11. Obrike, S. E. (2012). Evaluation of Imo clay-shale deposit (Paleocene) from Okada, Edo State, Southwestern Nigeria, as drilling mud clay. Journal of Applied Technology of Environmental Sanitation, 1(4), 311-316.
12. Nwajide, C. S. (2005). A guide to geological field trips to Anambra and related basins in Southeastern Nigeria. Great AP Express Publishers Ltd.
13. Okoye, I. P., & Obi, C. (2011). Synthesis and characterization of Al-pillared bentonite clay minerals. Research Journal of Applied Sciences, 6, 447-450.